1

Nucleation and Growth of Nanoparticles

Sulalit Bandyopadhyay[1] *and Seniz Ucar*[1,2]

[1] *Particle Engineering Centre, Department of Chemical Engineering, Norwegian University of Science and Technology, 7491 Trondheim, Norway*
[2] *Middle East Technical University, Department of Metallurgical and Materials Engineering, Üniversiteler, Dumlupınar Bulvarı No: 1, 06800 Ankara, Turkiye*

Nanomaterials display properties making them valuable for a broad range of applications ranging from energy production and storage to catalysis, biotechnology, sensing, and so on. Yet, to harness the desired properties effectively, it is essential to produce nanomaterials with precise control over size and shape, as these characteristics directly influence their behavior. Among various synthesis methods, crystallization is a widely utilized bottom-up approach for creating tailored inorganic nanoparticles (NPs). Crystallization refers to the formation of NPs as a result of first-order phase transition processes. During a spontaneous crystallization process, matter transforms from a higher free energy, disordered state into a crystalline state characterized by structural order and lower free energy. The gain in free energy as a result of crystal formation constitutes the thermodynamic driving force for crystallization and marks supersaturation as the first prerequisite and the key parameter controlling crystallization reactions and final particle properties. For crystallization to proceed from vapor, melt, or solution, the medium containing the solute must be supersaturated – an inherently nonequilibrium state that generates the excess free energy necessary to drive the crystallization process.

Crystallization comprises three successive stages: (i) the establishment of supersaturation, (ii) nucleation of particles, and (iii) particle growth. It is important to note that, depending on the reaction conditions, these stages may occur simultaneously within the crystallization medium. However, for the formation of each individual particle, the sequence of events follows the outlined order. Nucleation marks the initial step of particle formation in a supersaturated medium, representing the emergence of a new phase, i.e. phase separation, within the bulk. Following nucleation, growth leads to particle size enlargement, driven by the continued reduction of free energy as supersaturation is consumed. The important particle characteristics of solid phase, size, and shape are determined by the kinetics of nucleation and growth and by how the driving force is distributed between these processes.

Engineering Nanoparticles for Biomedical Applications: From Theory to Experiments and Modeling,
First Edition. Edited by Sulalit Bandyopadhyay.

The evolution of classical crystallization theory over the past century has provided a robust mathematical framework for predicting nucleation and growth rates. This framework has also enabled control over key crystal properties such as phase, size, uniformity, and morphology by highlighting the two principal factors governing crystallization processes: thermodynamics and kinetics. Thermodynamic factors, which constitute the driving force for nucleation and growth, dictate how material phases behave and crystallize in response to variables such as concentration, temperature, and pressure. In contrast, kinetic factors influence the rates of nucleation and growth, as well as the degree of crystal perfection and uniformity.

1.1 Classical Nucleation Theory

Classical nucleation theory (CNT), originally developed in the nineteenth century, explains nucleation as a dynamic and stochastic process where monomeric units – whether ions, atoms, or molecules – continuously coalesce and dissociate until they reach a critical size. At this critical size, a stable cluster, or nucleus, forms within the bulk, leading to phase separation. According to CNT, the thermodynamic basis for nucleation lies in the reduction of the system's free energy through the formation of a solid phase, with supersaturation serving as a prerequisite for spontaneous crystallization. This theory enables the derivation of a mathematical expression to quantify supersaturation, based on the chemical potential difference between the metastable (high free energy) and stable (low free energy) states of the system.

The chemical potential difference, $\Delta\mu$, between the two states of a system can be expressed as:

$$\Delta\mu = \mu_1 - \mu_2 \tag{1.1}$$

The chemical potential at any state, μ, is a function of the standard potential (μ_0), temperature (T), and activity of the solute (α):

$$\mu = \mu_0 + k_B T \ln a \tag{1.2}$$

where k_B is the Boltzmann constant. Combining these two equations, the thermodynamic driving force for spontaneous crystallization is found (Equation (1.3)), where α is the activity in an arbitrary state and α^* is the activity of the same solute at equilibrium.

$$\Delta\mu = k_B T \ln\left(\frac{a}{a^*}\right) \tag{1.3}$$

Supersaturation (S) is then defined as the ratio between the activities of the solute at two states and gives a measure of the thermodynamic potential of a system to form precipitates (Equation (1.4)):

$$S = \left(\frac{a}{a^*}\right) \tag{1.4}$$

The activity of a solute can be determined by considering all the reactions involving the solute within a reaction medium, which requires knowledge of the respective equilibrium constants. However, calculating activity may not be feasible

in multicomponent, complex systems. In such cases, solute concentration is often used as a substitute for activity, with the understanding that deviations will arise in nonideal solutions. These deviations are quantified by the activity coefficient, which accounts for the difference between the actual and ideal behavior of the solution.

Once a metastable system is achieved, i.e. supersaturation is established, nucleation can occur. Supersaturation provides the thermodynamic driving force necessary for nucleus formation. However, the phase separation of the nucleus within the bulk requires the creation of a surface, which incurs an energy cost. The overall Gibbs free energy change, ΔG, resulting from these two processes – the free energy change associated with the phase transformation, which scales with the volume of a nucleus (ΔG_{V}), and the free energy change associated with surface formation, which scales with the surface area (ΔG_{S}) – defines a critical size at which a stable nucleus can form in the system (Figure 1.1). When the total Gibbs free energy change is expressed as a function of the radius of a nucleus, assuming it is spherical, the critical size represents the thermodynamic energy barrier, or activation energy (ΔG_{crit} or ΔG^*), required for nucleation.

$$\Delta G = \Delta G_V + \Delta G_S = \frac{4}{3}\pi r^3 \Delta G_v + 4\pi r^2 \gamma \tag{1.5}$$

ΔG_{v} represents the chemical potential difference that induces the phase transformation and scales with supersaturation, where k_B is the Boltzmann constant, v_m is unit volume, and γ is the surface free energy of the nucleus-bulk interface.

$$\Delta G_v = -\frac{v k_B T \ln S}{v_m} \tag{1.6}$$

Combining Equations (1.5) and (1.6), and taking the first derivative of ΔG with respect to r, gives us the expression for ΔG^*:

$$\Delta G^* = \frac{16\pi\gamma^3 v_m^2}{3k_B^3 T^3 (\ln S)^2} \tag{1.7}$$

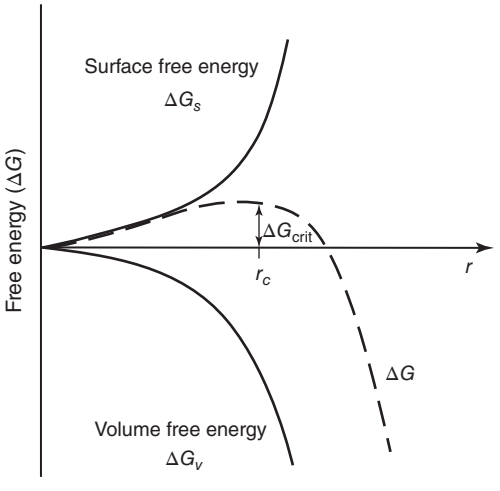

Figure 1.1 Schematic plot of total free energy change (ΔG) as a function of radius of nucleus (r), as a sum of two energy contributors, and the corresponding activation energy barrier (ΔG_{crit}). *Source*: [1] / The Royal Society of Chemistry.

Using the activation energy barrier for nucleation, an Arrhenius-type equation can be used to express nucleation rate, J:

$$J = A \exp\left[-\frac{\Delta G^*}{k_B T}\right] \tag{1.8}$$

The expression for the activation energy barrier highlights the key parameters that influence the energy requirement for nucleation and, consequently, the nucleation rate. These parameters include interfacial energy, temperature, and supersaturation. Additionally, the rate expression underscores the role of kinetic factors. As will be discussed later in this chapter, the ability to control the nucleation rate during crystallization is crucial for regulating particle size and size distribution.

The nucleation rate defines the number of nuclei that form per unit volume per unit time and is challenging to measure directly. In practice, induction time, t_{ind}, is used as an indirect measurement of nucleation rate, which is defined as the time interval between the formation of an appreciable amount of the solid phase and the establishment of supersaturation. Induction time is dependent on the sensitivity of the measuring method that is used to detect solid phase formation and thus cannot be considered as an intrinsic property of a crystallization system. Yet, induction time measurements are useful for the comparison of nucleation rates in similar experimental setups.

1.2 Phase Stability and Phase Transformations

For a given set of experimental conditions, such as composition and temperature, the solid phase with the lowest free energy is considered thermodynamically the most stable. All other phases that might exist under the same conditions are metastable in comparison. According to classical crystallization theory, the most stable phase forms from a supersaturated medium. However, this doesn't mean the system will directly transform into that stable phase. Instead, intermediate, metastable phases can emerge and persist in the system for significant periods.

When a solution is supersaturated with respect to multiple phases, each phase can nucleate at a certain rate defined by the kinetic parameters of nucleation and the associated activation energy barrier. Although the most stable phase generally has the lowest solubility and the highest supersaturation, metastable phases often have lower interfacial energies. This results in comparable effects of bulk and surface energies, and metastable phases can be associated with lower energy barriers. As particle size decreases, especially at the nanoscale, interfacial energy becomes comparable to the differences in phase stability, influencing which phases precipitate. Over time, these metastable phases will eventually transform into the stable phase, following Ostwald's rule of stages [2]. This rule suggests that systems often transition through intermediate phases before reaching the final stable phase, particularly when the stable phase has a high activation energy barrier for formation. Metastable phases exist at local energy minima and have the thermodynamic potential to transform into a more stable phase. The driving force for this transformation is the minimization of the system's total free energy, driven by the solubility difference between the stable and metastable phases.

1.3 Crystal Growth

Once nucleated, particles would subsequently grow provided that the system is supersaturated with respect to the nucleated phase. The morphology (external shape) of particles is determined during growth, and the diverse forms that particles can assume have practical significance for various applications. In the classical crystallization theory, size enlargement, i.e. crystal growth, occurs via continuous addition of building units. Based on this framework, we can explain morphology development from polyhedral crystals to dendrites and spherulites as a function of thermodynamic driving force and conduct quantitative analyses on growth kinetics with certain assumptions in place.

The driving force for growth is the lower chemical potential of the building units as they transition into solid constituents, moving the system toward equilibrium from a metastable state. Both nucleation and growth of particles are governed by the same thermodynamic driving force, which is defined by activity-based supersaturation. However, these two processes navigate different energy landscapes: growth is associated with a much lower activation energy barrier compared to nucleation. This difference is best illustrated by the LaMer diagram, where nucleation and growth dominate at different stages of a crystallization reaction as a function of supersaturation (Figure 1.2). The LaMer diagram depicts a crystallization process in which, after the initial burst of nucleation occurring above a critical supersaturation, the subsequent consumption of supersaturation is driven primarily by the growth of particles.

Crystal growth is a dynamic process where monomeric units must first diffuse from the bulk to the crystal surface and then incorporate into the crystal lattice. The rate and mechanism of growth are determined by the relative rates of these two processes and the microscopic characteristics of the crystal-bulk interface (Figure 1.3).

Growth mechanisms can be categorized based on the rate-limiting step: diffusion-controlled or surface reaction-controlled growth. When expressed mathematically, the effective parameters controlling growth rate and consequently particle size for these two mechanisms can be distinguished. In the case of diffusion-controlled

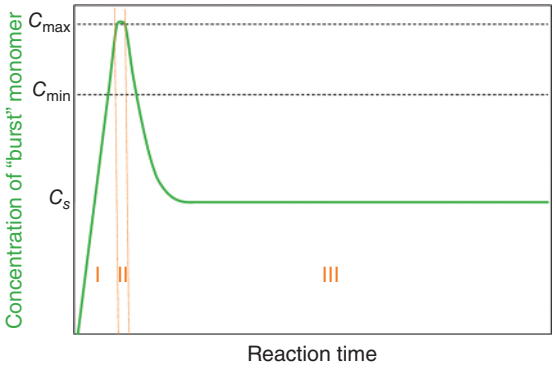

Figure 1.2 Schematic illustration of the LaMer model demonstrating establishment of supersaturation (zone I), leading to an instantaneous (burst) nucleation process (zone II) followed by particle growth (zone III). *Source*: [3] / American Chemical Society.

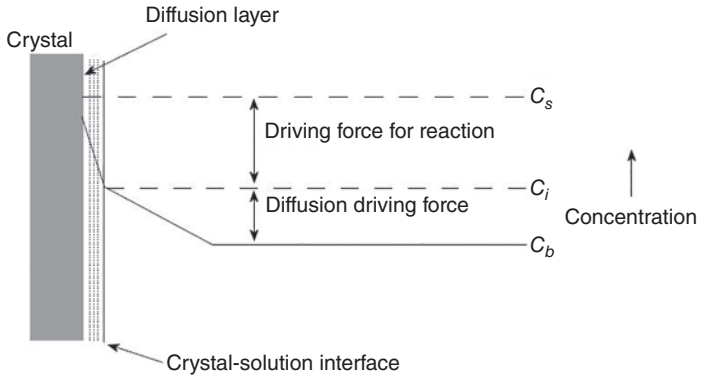

Figure 1.3 Concentration gradients of mass transfer between the bulk solution and crystal surface. *Source*: [4] / Baishideng Publishing Group Co.

growth of NPs, the growth rate shows a linear dependence on the flux of building units to the crystal surface, as described by Fick's first law:

$$\frac{dr}{dt} = DV_m \frac{dC}{dx} \tag{1.9}$$

where D is the diffusion coefficient, V_{m} is the molecular volume of the crystal, and C is the monomer concentration at distance x. As evident from Equation (1.9), in diffusion-controlled growth, the diffusion field surrounding a particle determines the growth rate. Another important implication of the significance of the concentration gradient on growth in the case of NPs is that at sufficiently small sizes, the solubility of NPs becomes a function of their size, with increasing solubility at smaller sizes. This size-dependent solubility drives the flux of monomers from smaller to larger particles, a phenomenon known as Ostwald ripening. Consequently, smaller particles dissolve, leading to the growth of larger ones at their expense [5].

In the case of surface reaction-controlled growth of NPs, the rate equation shows dependence on the rate constant for the surface reaction, k_{r}, and the concentration gradient at the interface between the diffusion layer and the crystal surface.

$$\frac{dr}{dt} = k_{\mathrm{r}} V_{\mathrm{m}} dC \tag{1.10}$$

In addition to the classical explanation of growth via monomeric attachment, particle-based growth models are also suggested for the formation of NPs. According to these models, supersaturation is eliminated during the initial formation of primary NPs, which later unite to form either single crystalline or polycrystalline particles [6]. The crystallographic orientation of the particles with respect to each other is proposed to be determined by the minimization of the free energy [7].

1.4 Control of Particle Size and Morphology

The performance of NPs is heavily influenced by factors such as size, size distribution, and shape/morphology, all of which are intricately controlled during their formation. A comprehensive understanding of the various stages of particle formation and the impact of reaction variables on these properties is essential for optimizing NPs for their intended use.

From a crystallization perspective, the nucleation stage plays a crucial role in determining the final size and size distribution of NPs. Crystal size is dictated by the interplay between nucleation and growth, both of which depend on the consumption of supersaturation in the system. High nucleation rates lead to the formation of numerous small particles, and if burst nucleation occurs within a short time frame under consistent conditions, the resulting particles will experience uniform subsequent growth. However, size distribution can still be modified during the growth process. Different growth mechanisms yield varying outcomes on size distribution, depending on the relationship between growth rate and particle size. Therefore, achieving uniformly sized NPs requires precise control over both nucleation and growth processes.

Regarding the morphology of NPs, the growth stage predominantly determines the final particle shape. The rate-limiting step of growth – whether it is governed by diffusion around the particles or by the incorporation rates of monomers into different crystal faces – can result in a wide range of morphologies, from faceted particles to branched and highly anisotropic shapes. The next section will delve into the control of particle size, size distribution, and morphology, using the principles of crystallization as a foundation.

1.4.1 Control of Size and Size Distribution of Spherical NPs

The activation energy barrier determines the probability of nucleation. As shown in Equation (1.7), the activation energy barrier is dependent on three factors: supersaturation, temperature, and interfacial energy. Out of these, the energy barrier changes most drastically with supersaturation. Figure 1.4 shows calculations for the nucleation rate as a function of these factors. It is evident that a change from $S = 2$ to $S = 4$ causes an increase in the nucleation rate of about $\sim 10^{70}$. However, while doing so, special concern should be given to stepwise precipitation pathways and phase transitions that can be induced under changing driving forces due to both thermodynamic and kinetic effects [8]. The nucleation rate may also be altered by changing the surface free energy. As an example, in hot-injection or heat-up synthesis of iron oxide NPs, by modifying the nature and concentration of the surfactant in the solution, the surface free energy may be adjusted so as to control the nucleation rate.

Using additives is another method to influence nucleation rate through altering solubility that is linked to supersaturation or adjusting the metastable zone width

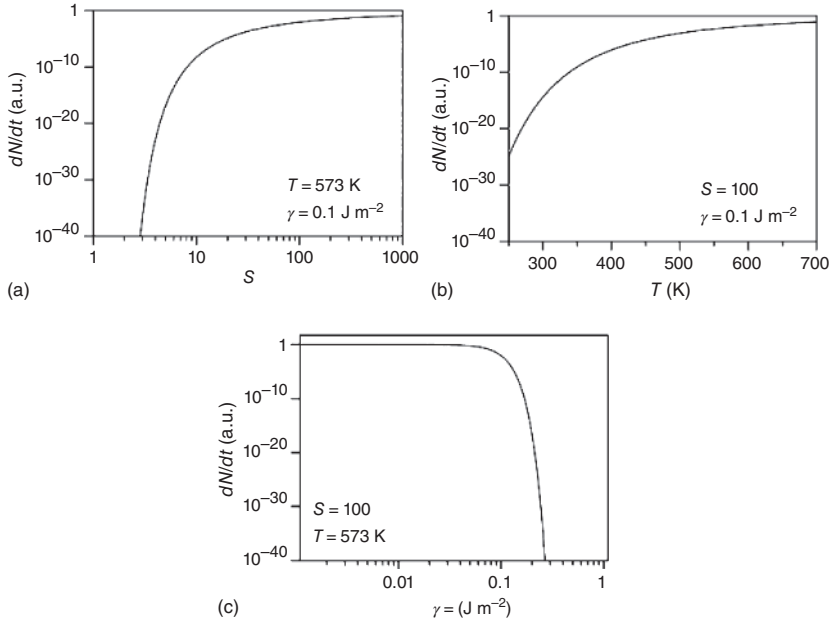

Figure 1.4 Nucleation rate as a function of supersaturation, temperature, and interfacial energy.

and/or nucleation induction time, both of which are closely related to interfacial tension and hence, nucleation rate. Thus, the presence of additives affects either the interfacial free energy or the kinetics of nucleation [9]. Promoted nucleation rates can be observed if the additives decrease the energy barrier for nucleation by offering heterogeneous nucleation sites and reducing the interfacial energy parameter. On the other hand, the presence of an additive might interfere with the kinetic factors of nucleation that are expressed in the pre-exponential factor, A, in the nucleation rate equation (Equation (1.8)). In the cases where additives cause repulsion forces, interfere with the incoming flux of monomers to the nuclei surface, or block the nucleation sites, their presence can lead to decreased nucleation rates.

A commonly used strategy to ensure the formation of small particles with narrow size distribution is burst nucleation, which refers to an experimental scheme that allows for intense nucleation during a short period of time without significant change in supersaturation, subsequently followed by growth. When nuclei are formed under constant conditions that provide a constant critical size and are subjected to similar growth conditions in terms of supersaturation and time of growth, a uniform size distribution is expected. On the other hand, if the nucleation continues during a time interval overlapping with the growth phase, a broader size distribution is obtained. However, it must be stressed that the particle size as well as size distribution are finalized during the size enlargement process.

Size enlargement or growth of the spherical NPs is largely governed by the supersaturation and, as mentioned earlier, is supported by two main growth theories:

classical growth that proceeds by monomeric attachment of growth units to the crystal surface as explained within the classical crystallization theory and particle-based pathways that rely on aggregation and self-assembly. In the former case, the growth of the NPs is further dependent on two mechanisms: the monomer's diffusion to the surface and the surface reaction. Depending on the mechanistic control, the size focusing effect, introduced earlier, namely Ostwald ripening, can influence the resultant size distribution. In the case where the surface reaction dominates, the size distribution will always be within the broadening regime, while for diffusion-controlled growth, under sufficiently high supersaturation, monodisperse particle size distribution is obtained. However, this self-sharpening effect becomes negligible as the particle size increases. Another formation step that controls particle size distribution is coagulation growth that happens via interparticle Brownian collision followed by complete fusion. This phenomenon not only depends on the radii of the colliding particles but also on solvent properties and surface functionalization of the particles, which govern the interparticle potential. Seeding is yet another approach to ensure that the supersaturation in the system is consumed in a controlled way. A small mass of crystals of interest is added to the supersaturated reaction medium to induce growth and secondary nucleation of the same phase [10].

Although solution supersaturation can display certain effects on the size and size distribution of NPs, effective kinetic control can also be established during the growth phase. Common methods employ the use of additives for this purpose, such as surfactants, ligands, polymers, or dendrimers, to confine the growth in the nanometer regime. Kinetic control may be easily achieved by spatially confining the growth, for example, inside micelles or in microemulsions, that not only ensures that growth stops when the limited amount of growth units is consumed or the available space is filled [11]. Another common approach is to employ capping agents, which are additives showing high affinity for the NP surface. Such capping agents influence the growth kinetics efficiently by blocking the active growth sites on the particle surface either temporarily or permanently and result in retardation or even complete inhibition of growth [12].

1.4.1.1 Example 1: Spherical Iron Oxide NPs

Co-precipitation of magnetite NPs is one of the most common methods of synthesis due to ease in scalability, high product purity, low-temperature requirements, water as a synthesis medium, and ease of in situ functionalization. A major drawback of the method is that it produces NPs with a broad size distribution [13, 14]. The method involves the precipitation of ferric (Fe^{3+}) and ferrous (Fe^{2+}) ions in the presence of a strong base such as NaOH or NH_4OH at moderate temperatures (<100 °C), and most commonly under an inert atmosphere [15]. Ravikumar recently showed that the various particle formation events that take place during the synthesis process provide the rationale for the formation of polydisperse NPs [16]. They estimated timescales of various individual particle formation events, namely (i) multiple Fe_3O_4 nucleation events, and several growth events such as (ii) diffusional-limited growth of primary and secondary nucleated particles, (iii) aggregation-based-coagulative growth of primary and secondary particles, and (iv) Ostwald ripening growth mechanism. These

estimated time scales were compared to the experimental aging time. The analysis revealed that the time scales associated with nucleation and various growth events, such as diffusional-limited and Ostwald ripening growth of small and large particles and coagulation of small particles, small and large particles, were all shorter than the experimental aging time. Consequently, these events were found to be completed within this time frame. However, the estimated time required for the coagulation of two large particles was longer than the experimental time, indicating that the formation of polydisperse Fe_3O_4 NPs in this route may be attributed to the incomplete coagulation of large particles and the successful completion of other growth events.

The main difficulties for effective control of magnetite synthesis stem from the low solubility of iron oxide minerals that results in highly supersaturated, labile solutions, which make decoupling nucleation and growth stages for efficient size control a challenge. In addition, iron oxide and (oxy)hydroxides can precipitate as several phases that differ in chemical composition and/or lattice structure, which necessitates designated reaction conditions to dictate precipitation of a target phase and further narrows the parameter window [17]. Kristiansen *et al*. showed stepwise precipitation of metastable iron oxide phases prior to magnetite formation via slow titration of a base (NaOH) into a solution of iron precursors (Fe^{3+} and Fe^{2+}) under an inert atmosphere [18]. A two-step formation pathway was observed, proceeding via the initial formation of ferrihydrite, followed by the precipitation of magnetite. However, the presence of an additive, PEG, led to the stabilization of the intermediate ferrihydrite phase, delaying magnetite formation. The effects of additives on the particle characteristics were associated with their ability to stabilize the intermediate iron hydroxide phases and affect the kinetics of phase transformation reactions.

1.4.1.2 Example 2: Spherical Au NPs

One of the most used syntheses of colloidal Au in aqueous solution is the reduction of tetrachloroauric acid ($HAuCl_4$) with trisodium citrate (Na_3Ct), popularly called the Turkevich method. The particle formation mechanism comprises four steps, as shown in Figure 1.5 [19]. The first step is a partial reduction of the Au precursor and the formation of small clusters from the Au monomers. In the second step, these clusters form seed particles with radii >1.5 nm. The remaining Au ions are attracted and attached in the electronic double layer (EDL) of the seed particles as co-ions. The third and fourth steps comprise the reduction of this ionic Au, first slowly and then

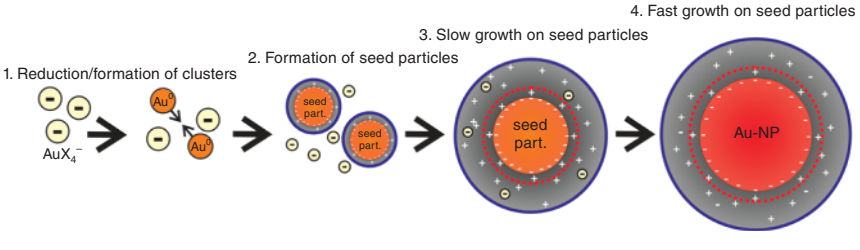

Figure 1.5 Particle formation mechanism in the Turkevich method for colloidal gold synthesis.

rapidly. The generated Au monomers grow exclusively on top of the seed particles' surfaces until the precursor is fully consumed, as a result of which, no new particles are formed during the last two steps. The described mechanism can be referred to as a seed-mediated growth mechanism, which can be distinguished clearly from a so-called nucleation growth mechanism, where the latter is based on the formation of "nuclei" – thermodynamically stable clusters, which, in general, consist of only a few atoms. In contrast, the growth mechanism described here is based on the formation of seed particles, which already have stable sizes and consist of some hundred atoms.

The final size of the Au NPs is already determined after the end of seed particle formation (after step 2 of the growth mechanism). The final total number of Au NPs is equivalent to the number of seed particles (since no new particle is formed after step 2) and determines to how many particles the total amount of available Au (directly dependent on initial $HAuCl_4$ concentration) is distributed. The number of seed particles is determined by the amount of Au monomers, which is available during the seed particle formation, while the minimum size of the seed particles determined by their colloidal stability. If more monomers are available, more seed particles can be formed, and the total amount of Au is distributed to more particles, leading to a smaller final size. If seed particles are stable at larger sizes, less particles can be formed from the available monomers, leading to larger final AuNP. These factors are determined by the reaction conditions since they influence either the reduction chemistry during seed particle formation, the colloidal stability of the seed particles, or both. Taking these two pathways into consideration, it is possible to understand and illustrate the influences of reaction conditions on the final NP size, which are controlled by the reactant concentrations, pH value, order of reactant addition, and synthesis temperature [20].

1.4.1.3 Example 3: Spherical Polymeric NPs

Polymeric NPs such as those of polystyrene and poly(lactic-*co*-glycolic) acid are synthesized using nanoprecipitation-based methods. Nanoprecipitation is based on the principle of mixing a polar organic solvent containing a polymer with an antisolvent (such as water), which is totally miscible with the organic solvent, thus creating supersaturation in the system. The organic phase may be mixed with the stirred aqueous phase in one shot, stepwise, dropwise, or by controlled addition rate, leading to the instantaneous formation of submicron spheres. To overcome an essential challenge of rapid mixing in the conventional nanoprecipitation, Prudhomme's group pioneered the use of efficient mixing cells to perform solvent-shifting in homogeneous conditions, the technique being called flash nanoprecipitation (FNP) [21]. A stream containing a molecularly dissolved polymer and stabilizing molecule is mixed fast with an opposing stream containing a miscible solvent, which acts as an anti-solvent for the solute and stabilizer, thereby providing the local supersaturation needed for particle nucleation [22]. Particle size in FNP can be modified through changing supersaturation levels by changing the polymer concentrations or the addition of co-precipitates that alter the nucleation process, resulting in a different particle size. Among other parameters, the solute solubility in the mixed solvent,

the ratio of organic solvent/water, the amount and nature of stabilizer, the nature of the polymer used, and the polymer molecular weight all influence the particle size and size distribution.

Supersaturation levels can be modified through changing the polymer concentration or the polymer solubility in the mixed solvent. The polymer concentration can be increased in the pre-mixed solvent stream through selecting water-miscible solvents affording high polymer solubility. A higher concentration represents a higher supersaturation, leading to high nucleation and growth rates, faster than the polymer aggregation rate. This provides additional time for particle growth before polymer stabilization, leading to larger particle sizes.

1.4.2 Control of Morphology of NPs

The morphology of a crystalline particle, manifested externally as the shape of the NP, is determined by two factors, namely the intrinsic characteristics of the crystal structure, which are the crystal lattice and the anisotropic bonding that constitutes the crystal structure, and the external factors of growth conditions, such as supersaturation and temperature. The final crystal morphology arises because of the relative growth rates of each of its faces, which is affected by both internal and external factors. In the end, the slow-growing faces become the largest, and the fast-growing faces become either small or disappear. For example, closely packed flat faces (F-faces) grow slower than stepped faces (S-faces) or kinked faces (K-faces), which means that in a growing crystal, F-facets will be exposed more and more, while S-faces and K-faces will gradually disappear [23].

If the internal factors alone controlled the particle morphology, the equilibrium morphology of the crystal at constant temperature and pressure would be the one that minimizes the total surface free energy, the so-called Wulff construction. For homogeneous nucleation, the shape of a (seed) crystal under equilibrium (thermodynamic) conditions can be predicted based on the Gibbs–Wulff theorem. This equilibrium shape is obtained by enclosing the crystal with the facets of the lowest possible surface energy as well as truncating the facets, leading to the minimum possible surface area for a given volume, which results in a polyhedron shape. In the case of heterogeneous nucleation, the seed can grow in an epitaxial or non-epitaxial way. In epitaxial growth, the deposited metal takes on a lattice structure and orientation identical to those of the substrate, and epitaxial growth happens when there exists a strong deposit–substrate interaction and a small lattice mismatch.

Another inherent factor that controls particle shape is the presence of twinning defects – a typical example of such crystals is face-centered cubic ones, which have low twin boundary energy. Twinned crystals are often elongated in one direction or flat; however, depending on the number of twin planes and relative growth rate of different facets, as determined by the kinetics, the multiply twinned particles may lead to, for example, decahedron-, star-, or right bipyramid-shaped particles.

Beside the inherent characteristics described earlier, the particle morphology depends highly on the external growth conditions and the resulting growth mechanism that is determined by supersaturation. As a rule of thumb, well-faceted

crystals are formed at low supersaturation, while rough surfaces are characteristics of the particle morphology at high supersaturation. To deepen the discussion, one can control anisotropic growth by exploiting the mechanism of crystal growth, from being surface-controlled to mass-transport limited. At or near equilibrium growth conditions, faces with the lowest surface energies dominate the crystal habit, as has been explained earlier. In crystals grown under surface-controlled conditions, faces with the slowest growth rate dominate the resulting habit, while for diffusion-controlled continuous growth conditions, the crystal habits tend to be rounded, as all crystal faces are rough and predicted to grow at the same rate. At very high supersaturations, morphological instability can occur, and dendritic, cellular, Hopper, etc., growth forms appear.

From a classification based on thermodynamic and kinetic growth control, it may be summarized that spherical, pseudo-spherical, or other isotropic NPs are usually formed if, during the growth process, the generated nuclei have a tendency to form low-energy NPs by supplying sufficient energy to the bulk solution or by having a low concentration of precursor monomer under thermodynamic control. On the other hand, the growth of nuclei driven by kinetic control leads to anisotropic shapes at high precursor monomer concentrations. Here, it must be clarified that the production and consumption rates of precursor monomer concentration have a strong influence on the nucleation and growth.

Supersaturation is controlled by the addition rate of the precursor monomer, the concentration of the reducing agent, and the ratio between the precursor and the reducing agent, among others. While the strength of the reducing agent has a direct influence on the supersaturation, higher reducing strength leads to higher supersaturation; in essence, the nature of the reducing agent is not effective in generating anisotropy in NPs. Solvents with different functional groups provide special coordination with the precursor monomer, which is advantageous for the formation process of NPs under both thermodynamic and kinetic control due to the adjustment of the supersaturation increase or depletion rate.

Another important factor, pH of the medium, also influences supersaturation by controlling the coordination bonding with other ions forming complexes, thereby promoting or postponing the release rate of ions (for supersaturation) influences the nucleation rate for shape control. In addition, pH also adjusts the surface properties of the preformed NPs and the chemical or physical state of the surfactants or additives, which are widely used to affect kinetic control [24, 25]. This may lead to different adsorption modes or adsorption amounts on the surface of the preformed NPs, resulting in selective growth or aggregation/agglomeration, and self-assembly, all of which favor the shape evolution of NPs. pH also has a decisive role for NPs with polymorphism, as it directly influences dissolution for phase transformation [26].

One of the most common ways of controlling NP shape is by employing additives, often referred to as capping agents, such as surfactants, ligands, or polymers, or exploiting the presence of impurities (foreign ions) in the reaction medium. Capping agents primarily change the relative growth rates of the facets through their interactions with particle surfaces, thereby inhibiting the incorporation rate of growth units onto the particle surfaces or changing the surface free energies of different facets or a

combination of both. The foreign ions in solution, such as metals and halides, generally adsorb on a certain set of facets of the growing particle more strongly than others. Such preferential adsorption affects the growth rate of a particle in an anisotropic fashion or may influence the formation of the defect structure of the seeds, resulting in the modification of the final crystal shape [27].

Finally, it may be noted that seeds or templates are also frequently used for shape control of NPs, and such a method is commonly referred to as the seed-mediated or template method. Such an approach is advantageous since the activation energy barrier for the addition of precursor monomers onto preformed seeds or templates is much lower compared with the formation of new nuclei from a homogeneous bulk solution [28, 29]. While the final shape of inorganic NPs generated using the template method is highly dependent on the initial shape of the template, the size of seeds should be extremely small (above critical size) as the final shape of the NPs is barely affected by the already formed shape of seeds but rather by a complex interplay of the seed amount, concentration of the precursor monomers, surfactants, temperatures, and so on [30, 31].

1.4.2.1 Example 1: Anisotropic Iron Oxide NPs

Magnetite NPs are most often found as cubes or octahedrons, as these shapes are compatible with the symmetry of the spinel structure (cubic). Co-precipitation and thermal decomposition are the two most common methods for synthesizing magnetite iron oxide nanoparticles (IONPs), while the former uses mostly water as the reaction medium, the latter employs high boiling organic solvents. The literature reports two main strategies to grow cubic magnetic NPs – one that deals with fixed experimental conditions and the other with the use of ligands with specific affinity to (100) faces [32].

A study by Verges et al. reports the preparation of uniform magnetite NPs with sizes around 30 nm and stable in aqueous media at pH 7 based on the precipitation of an iron (II) salt ($FeSO_4$) in the presence of a base (NaOH) and a mild oxidant (KNO_3) [33]. The reaction rate seems to be controlled by the iron salt concentration and the presence of ethanol in the media. The authors reported the most critical parameter to be [Fe(II)]:2[OH^-] ratio: 33 nm nanocubes were achieved when the ratio was 0.77, and when the ratio got closer to 1, larger sizes were obtained, with the particle shape evolving to octahedral morphology (Figure 1.6). The reaction kinetics is affected by the pH and how far/close it is from the isoelectric point of magnetite. It was reported that in excess of OH^-, i.e. when the pH was above the Fe_3O_4 isoelectric point, cubic particles grew by slow diffusion of $Fe(OH)_2$ species to the primary particles (negatively charged). However, without an excess of OH^-, the kinetics of growth is faster and happens mainly by aggregation. Since, under these conditions, the primary particles are not sufficiently charged, there are inadequate repulsive forces. The aggregation is followed by subsequent recrystallization, leading to octahedral particles with larger sizes ranging from a few nanometers up to microns. The authors also reported that the addition of ethanol induces the cubic morphology as well and reduces the final size of the particles. Such observations are traced back to the modification of the hydrolysis of ferrous and ferri oxo-aqueous

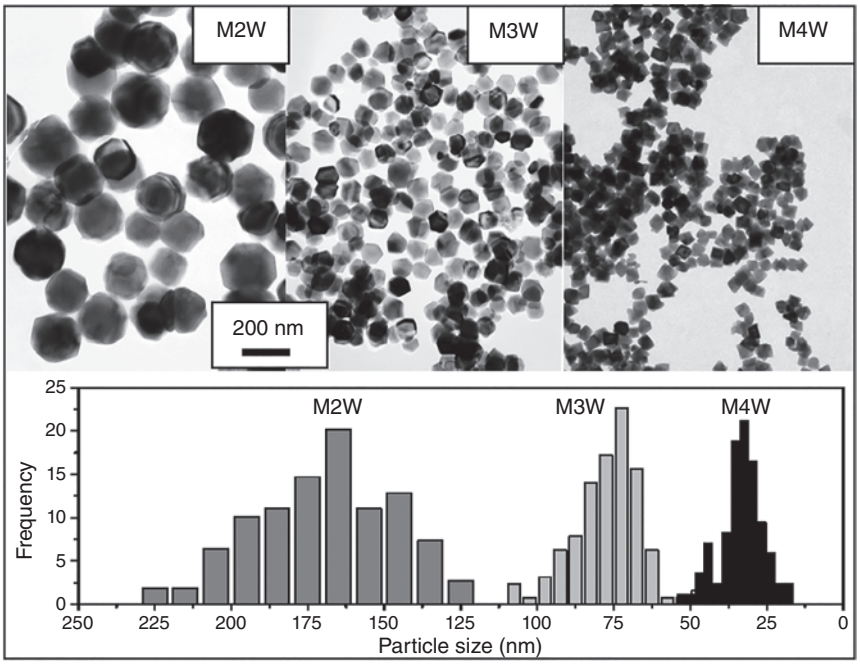

Figure 1.6 TEM images and histograms for magnetite nanoparticles synthesized at different Fe (II) concentrations. M2W, M3W, and MW4 are synthesized with different ratios of [Fe(II)]:2[OH^-], i.e. 0.997, 0.97, and 0.77, respectively, yielding average sizes of 169, 76, and 33 nm, respectively. With increasing values of the ratio, the particle shape transitions from cubic to octahedral. *Source*: [34] / IOP Publishing.

species, decreasing the critical diameter at which nuclei can be formed, and finally slowing down the growth, hampering the diffusion process.

In a thermal decomposition route, the particle size can be tailored by changing both the precursor concentration and reflux time, or the heating rate, or the solvent, or a combination of all these. It is important to note that the nature of the surfactants has a decisive control on the final morphology of the IONPs. Kovalenko et al. showed that the addition of sodium or potassium oleate in the thermal decomposition of the iron oleate precursor leads to cubic nanocrystals between 9 and 23 nm. However, when the surfactant was replaced by oleic acid or dibutyl ammonium oleate, spherical NPs were grown. The cubical shape of the NCs was hypothesized to be a result of a slower growth rate for the {100} facets as compared to all other facets [35]. The authors attribute the anisotropy of the growth rate to a different adhesion of the stabilizer on the growing surface, since the stabilizer species was the only parameter, which was changed to obtain cubical shapes instead of spheres.

1.4.2.2 Example 2: Anisotropic Au NPs

Anisotropic Au NPs find wide applications within biomedicine and catalysis owing to their shape-dependent optical properties. For example, in the field of biomedicine, larger Au nanorods might provide better performance in optical

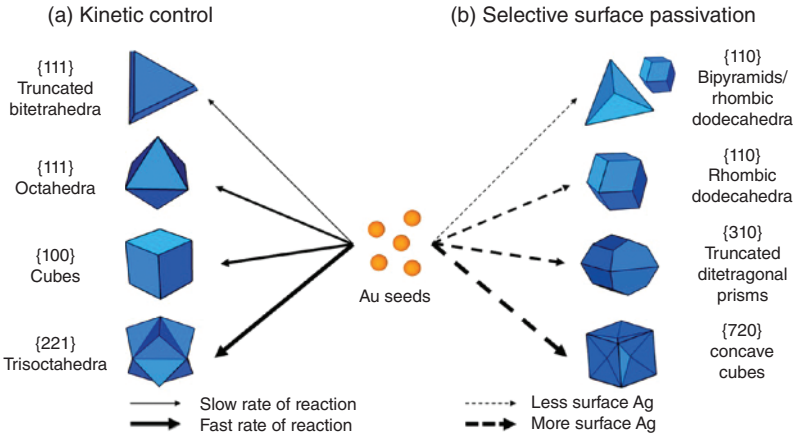

Figure 1.7 Growth pathways for anisotropic gold nanoparticles: kinetic control and selective surface passivation.

imaging applications, whereas smaller Au nanorods might provide improved efficiency in photo-thermal therapy applications that function by converting incoming photons into outgoing heat because of their improved absorption efficiency [36]. The seed-mediated synthesis of Au NPs is the most common method to synthesize anisotropic structures. The method can be divided into two main synthetic steps: (i) the rapid reduction of Au ions to form small, highly monodisperse, surfactant-coated spherical Au NPs, or seeds, and (ii) the growth of larger NPs by slowly reducing additional Au onto the previously synthesized seeds (which serve as nucleation sites) in the presence of shape-directing additives. The formation of anisotropic Au NPs predominantly follows one of two growth pathways, as shown in Figure 1.7: (i) kinetic control or (ii) selective surface passivation. Under kinetic control, the rate of Au^{+} reduction directs NP shape, while in the selective surface passivation pathway, the deposition of Ag onto the Au NP surface blocks the growth of particular facets and thus dictates NP shape. To unravel the mayhem behind the shape control of Au NPs, Personik and Mirkin have summarized the mechanisms that control Au NP shape via these pathways in the context of three variables: metal complex reduction potential, metal ion availability, and adsorbate binding strength. These factors influence the crystallinity and surface facets of the Au NPs, thus dictating particle shape [37].

1.5 Concluding Remarks

The performance of NPs is profoundly influenced by their size, size distribution, and morphology – attributes that are intricately shaped during their formation. A thorough understanding of the stages of particle formation, particularly the nucleation and growth processes, is crucial for optimizing these properties. The nucleation stage is especially pivotal, as it sets the foundation for the final size and distribution of NPs, while the growth stage largely dictates their morphology.

Achieving a uniform size distribution and desired morphology in NPs requires precise control over the conditions that govern nucleation and growth. By mastering these processes, it is possible to tailor NPs for specific applications, enhancing their performance and functionality. The intricate balance between thermodynamic and kinetic factors during crystallization, along with the ability to manipulate reaction variables, provides a powerful toolkit for the design and synthesis of NPs with targeted properties. As the field of nanotechnology continues to advance, the insights gained from studying the crystallization behavior of NPs will be instrumental in developing new materials with enhanced capabilities, opening the door to a wide range of applications across various industries.

References

1 Myerson, A.S. (2015). Concluding remarks. *Faraday Discussions* 179: 543–547. https://doi.org/10.1039/C5FD00042D.

2 Jeurgens, L.P., Wang, Z., and Mittemeijer, E.J. (2009). Thermodynamics of reactions and phase transformations at interfaces and surfaces. *International Journal of Materials Research* 100 (10): 1281–1307.

3 Whitehead, C.B., Özkar, S., and Finke, R.G. (2019). LaMer's 1950 model for particle formation of instantaneous nucleation and diffusion-controlled growth: a historical look at the model's origins, assumptions, equations, and underlying sulfur sol formation kinetics data. *Chemistry of Materials* 31 (18): 7116–7132.

4 Dorozhkin, S.V. (2012). Dissolution mechanism of calcium apatites in acids: a review of literature. *World Journal of Methodology* 2 (1): 1.

5 Shtukenberg, A.G., García-Ruiz, J.M., and Kahr, B. (2021). Punin ripening and the classification of solution-mediated recrystallization mechanisms. *Crystal Growth & Design* 21 (2): 1267–1277.

6 Ivanov, V.K., Fedorov, P.P., Baranchikov, A.Y., and Osiko, V.V.E. (2014). Oriented attachment of particles: 100 years of investigations of non-classical crystal growth. *Russian Chemical Reviews* 83 (12): 1204.

7 Yuwono, V.M., Burrows, N.D., Soltis, J.A., and Penn, R.L. (2010). Oriented aggregation: formation and transformation of mesocrystal intermediates revealed. *Journal of the American Chemical Society* 132 (7): 2163–2165.

8 Kwon, S.G. and Hyeon, T. (2011). Formation mechanisms of uniform nanocrystals via hot-injection and heat-up methods. *Small* 7 (19): 2685–2702.

9 Xu, S., Cao, D., Liu, Y., and Wang, Y. (2021). Role of additives in crystal nucleation from solutions: a review. *Crystal Growth & Design* 22 (3): 2001–2022.

10 Bachhar, N. and Bandyopadhyaya, R. (2016). Predicting complete size distribution of nanoparticles based on interparticle potential: experiments and simulation. *The Journal of Physical Chemistry C* 120 (8): 4612–4622.

11 Thanh, N.T., Maclean, N., and Mahiddine, S. (2014). Mechanisms of nucleation and growth of nanoparticles in solution. *Chemical Reviews* 114 (15): 7610–7630.

12 Javed, R., Zia, M., Naz, S. et al. (2020). Role of capping agents in the application of nanoparticles in biomedicine and environmental remediation: recent trends and future prospects. *Journal of Nanobiotechnology* 18: 1–15.

13 Lu, A.H., Salabas, E.E., and Schüth, F. (2007). Magnetic nanoparticles: synthesis, protection, functionalization, and application. *Angewandte Chemie International Edition* 46 (8): 1222–1244.

14 Lu, A.H., Salabas, E.E., and Schüth, F. (2007). Magnetic nanoparticles: synthesis, protection, functionalization, and application. *Angewandte Chemie International Edition* 46 (8): 1222–1244.

15 Massart, R. (1981). Preparation of aqueous magnetic liquids in alkaline and acidic media. *IEEE Transactions on Magnetics* 17 (2): 1247–1248. https://doi.org/10.1109/TMAG.1981.1061188.

16 Ravikumar, C. (2023). Unveiling the formation mechanism of polydisperse iron oxide nanoparticles in coprecipitation route. *Journal of Crystal Growth* 624: 127419.

17 Cornell, R.M. and Schwertmann, U. (2003). *The Iron Oxides: Structure, Properties, Reactions, Occurrences, and Uses*, vol. 664. Weinheim: Wiley-VCH.

18 Kristiansen, A.B., Church, N., and Ucar, S. (2023). Investigation of magnetite particle characteristics in relation to crystallization pathways. *Powder Technology* 415: 118145.

19 Polte, J. (2015). Fundamental growth principles of colloidal metal nanoparticles – a new perspective. *CrystEngComm* 17 (36): 6809–6830.

20 Wuithschick, M., Birnbaum, A., Witte, S. et al. (2015). Turkevich in new robes: key questions answered for the most common gold nanoparticle synthesis. *ACS Nano* 9 (7): 7052–7071.

21 Sulalit, B. and Mani, E. (2023). Chapter Three – Design and modeling of sub-micron particles via precipitation. In: *Advances in Chemical Engineering* (eds. E. Mauri, and Z.J. Zhang), Vol. 62, 59–91, Academic Press, ISSN 0065-2377, ISBN 9780443218668, https://doi.org/10.1016/bs.ache.2023.10.005.

22 Saad, W.S. and Prud'homme, R.K. (2016). Principles of nanoparticle formation by flash nanoprecipitation. *Nano Today* 11 (2): 212–227.

23 Sau, T.K. and Rogach, A.L. (2010). Nonspherical noble metal nanoparticles: colloid-chemical synthesis and morphology control. *Advanced Materials* 22 (16): 1781–1804.

24 Harn, Y.W., Yang, T.H., Tang, T.Y. et al. (2015). Facet-dependent photocatalytic activity and facet-selective etching of silver (I) oxide crystals with controlled morphology. *ChemCatChem* 7 (1): 80–86.

25 Papadopoulou, E. and Bell, S.E. (2010). Structure of adenine on metal nanoparticles: pH equilibria and formation of Ag^+ complexes detected by surface-enhanced Raman spectroscopy. *The Journal of Physical Chemistry C* 114 (51): 22644–22651.

26 Alqadi, M.K., Abo Noqtah, O.A., Alzoubi, F.Y. et al. (2014). pH effect on the aggregation of silver nanoparticles synthesized by chemical reduction. *Materials Science-Poland* 32: 107–111.

27 Aherne, D., Ledwith, D.M., Gara, M., and Kelly, J.M. (2008). Optical properties and growth aspects of silver nanoprisms produced by a highly reproducible and rapid synthesis at room temperature. *Advanced Functional Materials* 18 (14): 2005–2016.

28 Lin, Z.J., Chen, X.M., Cai, Z.M. et al. (2008). The initial transformation mechanism of gold seeds on indium tin oxide surfaces. *Crystal Growth and Design* 8 (3): 863–868.

29 Fan, F.R., Liu, D.Y., Wu, Y.F. et al. (2008). Epitaxial growth of heterogeneous metal nanocrystals: from gold nano-octahedra to palladium and silver nanocubes. *Journal of the American Chemical Society* 130 (22): 6949–6951.

30 Huang, C.C., Yang, Z., and Chang, H.T. (2004). Synthesis of dumbbell-shaped Au–Ag core–shell nanorods by seed-mediated growth under alkaline conditions. *Langmuir* 20 (15): 6089–6092.

31 Xu, Z.C., Shen, C.M., Xiao, C.W. et al. (2007). Wet chemical synthesis of gold nanoparticles using silver seeds: a shape control from nanorods to hollow spherical nanoparticles. *Nanotechnology* 18 (11): 115608.

32 Roca, A.G., Gutiérrez, L., Gavilán, H. et al. (2019). Design strategies for shape-controlled magnetic iron oxide nanoparticles. *Advanced Drug Delivery Reviews* 138: 68–104.

33 Vergés, M.A., Costo, R., Roca, A.G. et al. (2008). Uniform and water stable magnetite nanoparticles with diameters around the monodomain–multidomain limit. *Journal of Physics D: Applied Physics* 41 (13): 134003.

34 Vergés, M.A., Costo, R., Roca, A.G. et al. (2008). Uniform and water stable magnetite nanoparticles with diameters around the monodomain–multidomain limit. *Journal of Physics D: Applied Physics* 41 (13): 134003.

35 Kovalenko, M.V., Bodnarchuk, M.I., Lechner, R.T. et al. (2007). Fatty acid salts as stabilizers in size-and shape-controlled nanocrystal synthesis: the case of inverse spinel iron oxide. *Journal of the American Chemical Society* 129 (20): 6352–6353.

36 Lohse, S.E. and Murphy, C.J. (2013). The quest for shape control: a history of gold nanorod synthesis. *Chemistry of Materials* 25 (8): 1250–1261.

37 Personick, M.L. and Mirkin, C.A. (2013). Making sense of the mayhem behind shape control in the synthesis of gold nanoparticles. *Journal of the American Chemical Society* 135 (49): 18238–18247.